

ARTIGO

STUDY OF THE OPTICAL PROPERTIES OF TeO₂-PbO-TiO₂ GLASS SYSTEM

Raul F. Cuevas, Ana M. de Paula, Carlos L. Cesar e Luiz C. Barbosa

Instituto de Física - Universidade Estadual de Campinas - CP 6165 - 13083-970 - Campinas-SP

Oswaldo L. Alves

Instituto de Química - Universidade Estadual de Campinas - CP 6154 - 13083-970 - Campinas-SP

Recebido em 2/12/96; aceito em 18/2/97

We describe the preparation and some optical properties of high refractive index TeO₂-PbO-TiO₂ glass system. Highly homogeneous glasses were obtained by agitating the mixture during the melting process in an alumina crucible. The characterization was done by X-ray diffraction, Raman scattering, light absorption and linear refractive index measurements. The results show a change in the glass structure as the PbO content increases: the TeO₄ trigonal bipyramids characteristics of TeO₂ glasses transform into TeO₃ trigonal pyramids. However, the measured refractive indices are almost independent of the glass composition. We show that third-order nonlinear optical susceptibilities calculated from the measured refractive indices using Lines' theoretical model are also independent of the glass composition.

Keywords: tellurite glass; non-linear glasses; high refractive index glass.

INTRODUCTION

Tellurium oxide based glasses are potential materials for optical device applications due to their nonlinear optical properties. They show high refractive index, and consequently high third order nonlinear susceptibility $\chi^{(3)}$, and high dielectric constant^{1,2}. Also, they are transparent over the visible and near infrared regions. Kim *et al*³ have measured for a pure TeO₂ glass a value of $\chi^{(3)}=1.41 \times 10^{-12}$ esu, however it is not easy to obtain this pure glass. Some recent works have shown that the addition of TiO₂.PbO and Nb₂O₅ increases the glass stability and refractive index⁴⁻⁷. In particular, the TeO₂-PbO-TiO₂- glass system have presented the highest $\chi^{(3)}$ values, in the range from 2×10^{-12} to 4×10^{-12} esu^{5,6}. Nonetheless, the dependence of the nonlinear properties on the concentration of the three components is not yet clearly established. The discrepancies in the measured $\chi^{(3)}$ values are still quite high, probably due to inhomogeneities in the glass^{5,6}.

In this work we present a study of the properties of this glass system as a function of the PbO composition. We have synthesised (90-x)TeO₂:xPbO:10TiO₂ glasses with x=5, 10, 15, 20 and 25 mol%. We obtained high homogeneous glasses by agitating the mixture during the melting process. The glasses were characterized by means of X-ray diffraction (XRD), Raman scattering, optical absorption and linear refractive index measurements. Most of the measured properties show the already observed^{6,8} change in the glass structure as the PbO content increases: the TeO₄ trigonal bipyramids characteristics of TeO₂ glasses break into the TeO₃ trigonal pyramids. Nonetheless, the measured refractive indices are almost independent of the glass composition. Calculated $\chi^{(3)}$ values

using Lines' theoretical model^{9,10} are also independent of the glass composition

EXPERIMENTAL

We studied a series of five (90-x)TeO₂:xPbO:10TiO₂ glass samples with 5, 10, 15, 20 and 25 mol%, which we denote as PTT1, PTT2, PTT3, PTT4, and PTT5, respectively (see Table 1). The materials used were reagent grade TiO₂ (from Merck), TeO₂ (from Merck) and PbO (from Riedel). A bath of 25 grams of the mixture for each composition was placed directly in an alumina crucible in an electric furnace. The mixture was agitated during the melting process in order to obtain homogeneous concentrations. Melting was achieved at a temperature of 900°C for 20 minutes. The melt was quenched between a pair of stainless steel plates and later annealed for 2 hours at 300°C. The samples were prepared in two forms: powder for the XRD, and approximately 1 mm thick slabs for the other measurements.

The glassy state was confirmed by X-ray diffraction analysis using CuK α radiation in a Shimadzu diffractometer. The Raman spectra were measured using the argon ion laser line at 514.5 nm at backscattering geometry and a triple Jobin-Yvonspectrometer with multichannel detection. The absorption measurements were obtained using a Perkin-Elmer Lambda 9 spectrophotometer.

For the refractive index measurements we used a manual Rudolph null ellipsometer (model 436) with a 150 W tungsten lamp as a light source. The desired wavelengths were selected by interference filters. The output power of the ellipsometer optics was measured with a commercial liquid-nitrogen-cooled InAs detector, whose signal was integrated by a lock-in

Table 1. Parameters used in the $\chi^{(3)}$ calculations and the obtained values considering $f = 1.72$.

Glass	Composition (mol %)	n at 1.907 μm	f_L	E_o (eV)	I_d (\AA)	$\chi^{(3)}$ (10^{-12} esu)
PTT1	5PbO-10TiO ₂ -85TeO ₂	1.871	1.834	4.87	1.923	3.49
PTT2	10PbO-10TiO ₂ -80TeO ₂	1.850	1.808	4.73	1.932	3.48
PTT3	15PbO-10TiO ₂ -75TeO ₂	1.854	1.813	4.75	1.942	3.54
PTT4	20PbO-10TiO ₂ -70TeO ₂	1.855	1.814	4.78	1.952	3.54
PTT5	25PbO-10TiO ₂ -65TeO ₂	1.854	1.813	4.73	1.962	3.63

amplifier. The use of a less noisy detector instead of the cooled PbS detector supplied by the manufacturer has proved to be essential to achieve the experimental errors of 0.1%.

RESULTS AND DISCUSSIONS

Glass Formation

The preparation procedure described in the experimental permitted us to obtain bubble free transparent glasses with high homogeneity and a yellowish colour. All the compositions showed the XRD patterns typical for a glass phase presenting an halo near $2\theta=22,5^\circ$.

Raman Spectra

The Raman spectra from the PTT glasses are presented in figure 1. We have observed the following features in the spectra: a band at 135 cm^{-1} which is assigned to the PbO vibrations⁸, a broad band around 478 cm^{-1} which is assigned to Te-O-Te bending modes¹¹, whose intensity decreases as the PbO content increases. The two bands observed around 682 and 773 cm^{-1} have been assigned to the stretching vibrations of TeO_4 trigonal bipyramids, characteristics of TeO_2 glasses, and stretching vibrations of the TeO_3 trigonal pyramids, respectively^{8,11}. Note that as the PbO content increases the intensity of the TeO_3 band increases with relation to that of the TeO_4 band, and the TeO_3 band is the most intense band for the samples PTT4 and PTT5. Also these bands shift slightly to lower Raman energy as the PbO concentration increases. There is also a weak band at about 300 cm^{-1} for PbO contents greater than 15 mol% which has been assigned to the bending vibrations of TeO_3 trigonal pyramids with non-bridging oxygen. These results are consistent with the structural change observed for PbO: TeO_2 glass systems, as the PbO content increases the TeO_4 trigonal bipyramids break into TeO_3 trigonal pyramids. Nonetheless this change is slower when compared to $\text{Li}_2\text{O}:\text{TiO}_2:\text{TeO}_2$ glasses⁷. Yamamoto *et al*⁵, presented quantitative measurements of the Te coordination number in these two glass systems that showed this same trend.

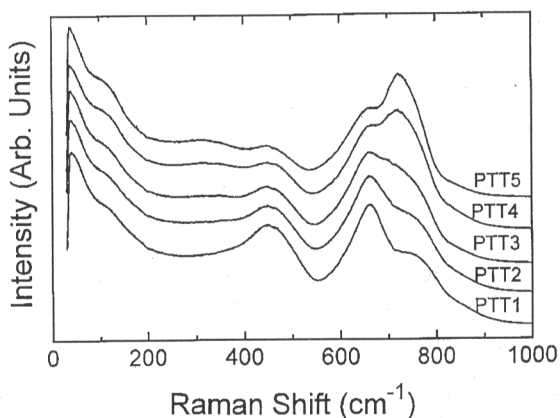


Figure 1. Raman spectra of the PTT glass system. The spectra were arbitrarily shifted vertically for clarity.

Optical Absorption

We have measured the glass transmission in the wavelength range 250 to 1500 nm. The transmittance are shown in the inset of figure 2 for the samples PTT1 and PTT2, the curves are almost flat from 800 to 1500 nm. The curves for the other samples (PTT3 to PTT5) are indistinguishable from the PTT2 curve. The UV-Vis cut-off wavelength is at about 420 nm for all compositions.

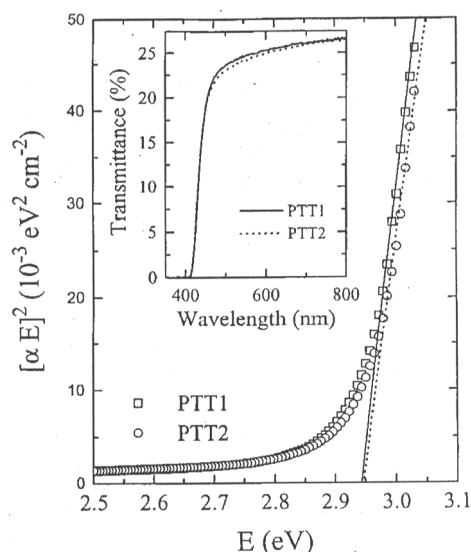


Figure 2. Plot of $(\alpha E)^2$ as a function of energy for the PTT glass system, the curves for the PTT3, PTT4 and PTT5 glasses are indistinguishable from the curve for the PTT2 glass. The solid and dashed lines are the linear fits to obtain the optical gap for PTT1 and PTT2 samples, respectively. The inset shows the transmission curves.

From the transmission curve we calculated the optical absorption coefficient α . In order to obtain the optical energy gap we plotted $(\alpha E)^2$ as a function of energy E , figure 2 shows the curves for the samples PTT1 and PTT2. The values of the optical energy gap were obtained from the extrapolation of the linear regions of the plots to $(\alpha E)^2 = 0$. The optical gap is at about 2.94 eV for all the PbO compositions.

Linear Refractive Index

We have measured the linear refractive index, n , of the glasses for wavelengths centred at 546, 633, 800, 1300, 1750 and 2000 nm. The bandwidth of the used filters was of 70 nm. The values are listed in table 2, the experimental errors are about 0.1%. The figure 3 shows the linear refractive index dispersion, the solid lines are extrapolation curves. In figure 4 we plot the refractive index as a function of PbO content for all the measured wavelengths. Note that there is just a small change with the PbO content: the values for the PTT1 sample are slightly larger than for the other samples, at the high wavelength region. Also plotted in figure 4 are the linear refractive index data at 632.8 nm (crosses) from Yamamoto *et al*⁶. The values are comparable, however their results show an increasing trend with PbO content which we do not observe.

We have calculated E_d and E_o using the expression for n as a function of the energy E proposed by Wemple¹²: $1/(n_2-1) = E_o/E_d - E^2/E_o E_d$, where E_o is the average excitation energy for electronic transition and E_d is the electronic oscillator strength related to dispersion. The E_o values (listed in table 1) will be used to calculate the nonlinear refractive index.

Nonlinear Refractive Index

To calculate the nonlinear refractive index we used Lines' bond-orbital theory^{9,10}, that considers the influence of cationic empty d -orbital on the glass nonlinear optical response. The contribution of the d -orbital to the nonlinear response is proportional to the decrease of the bond length between cation and anion l_d and to the increase of the orbitals overlap $\langle d|p \rangle$. He studied a number of transparent transition-metal oxides and found that this contribution is negligible for bond lengths $l_d > 2.3\text{ \AA}$, but increases rapidly as the bond length decreases and becomes

Table 2. Measured refractive index as function of wavelength for the PTT glasses.

Wavelength (nm)	n PTT1	n PTT2	n PTT3	n PTT4	n PTT5
546	2.204	2.209	2.208	2.207	2.208
633	2.150	2.152	2.153	2.151	2.152
800	2.088	2.085	2.085	2.086	2.084
1300	1.990	1.981	1.983	1.981	1.983
1750	1.907	1.891	1.892	1.893	1.892
2000	1.852	1.835	1.835	1.836	1.834

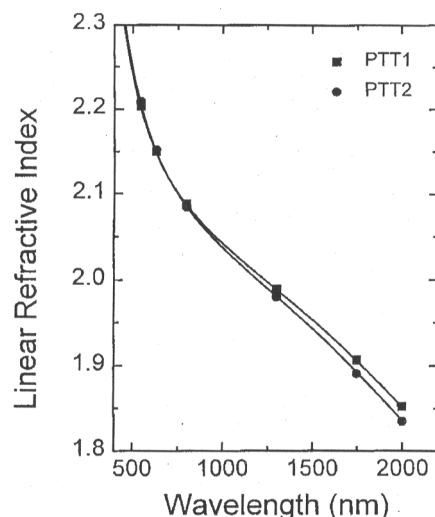


Figure 3. Linear refractive index as a function of the wavelength for the PTT glass system. The squares are for the PTT1 sample and circles for the PTT2. The results for the PTT3, PTT4 and PTT5 are indistinguishable from those for the PTT2 glass. The lines are extrapolation curves.

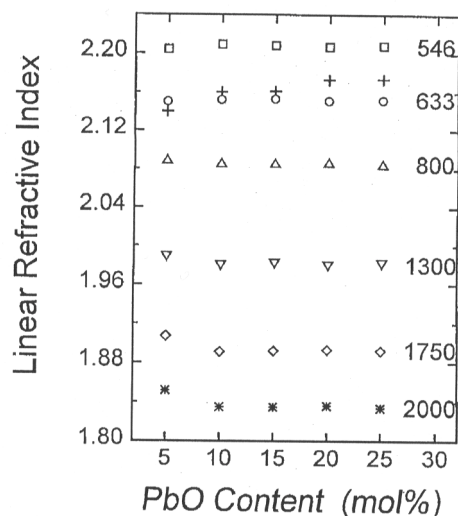


Figure 4. The linear refractive index of the PTT glass system as a function of the PbO content. The wavelengths in nm are indicated at the right side of the plot. The crosses are the data of Yamamoto *et al*⁶.

dominant for $l_d < 2.0 \text{ \AA}$. The nonlinear optical response was obtained using a variational method to describe the effect of an applied electric field fE_x along the bond direction x in the perturbed molecular orbital. The factor f takes in account any local field enhancement or shielding effects. The frequency dependent nonlinear refractive index n_2 is expressed by the empirical formula¹⁰:

$$n_2(av) = \frac{25f^3 f_L^3 l_d^2 (n^2 - 1) E_s^6}{n(E_s^2 - \hbar^2 \omega^2)^4} (10^{-13} \text{ esu}) \quad (1)$$

where $f_L = (n^2 + 2)/3$ is the Lorentzian local field enhancement factor⁹, n is the long-wavelength limit value of the refractive index, E_s in eV is the effective Sellmeier energy gap which takes in account the contributions of the sp and d orbitals, and l_d in \AA is the bond length for the ternary glass. The Sellmeier gap is in practice equal to E_0 in Wemple's equation¹², values are listed in table 1. The bond lengths for the ternary glasses were estimated using the method proposed by Nassau¹³, with the Pb-O, Ti-O and Te-O bond lengths as 2.24 \AA , 1.96 \AA and 1.91 \AA , respectively¹⁰. Also, we use the following equation⁹ to convert n_2 into $\chi^{(3)}$:

$$\chi^{(3)}(-3\omega, \omega, \omega, \omega) = \frac{n}{3\pi} n_2(av) (esu) \quad (2)$$

The estimated $\chi^{(3)}$ at the wavelength of 1.907 μm (the wavelength for the measured data of Yamamoto *et al*⁶) are given in table 1 and plotted in figure 5 (circles), for the PTT glasses. Note that the results are almost independent of the PbO content. To compare our results with the data of Yamamoto *et al*⁶ (triangles) we have used $f=1.72$, we chose to make the values of $\chi^{(3)}$ equal to the experimental value for the PbO content of 25 mol%. This f value is close to the value of 1.9 ± 0.1 obtained by Lines¹⁰ for transition-metal oxides dominated by d -band response. This is an indication that Lines' model, which assumes that the high nonlinear optical response is due to virtual excitations from the cationic sp levels to virtual d levels, is valid for TeO_2 based glasses. Kim *et al*³ have already shown that this model can be used for a TeO_2 pure glass, where the most probable optical transition is the electron transfer from $2p\pi$ orbitals of the Oxygen to the empty non-bonding $5d$ orbitals of Tellurium. We have also shown that this model holds for the $\text{Li}_2\text{O}:\text{TiO}_2:\text{TeO}_2$ glass system⁷.

It should be pointed out that for the $\text{Li}_2\text{O}:\text{TiO}_2:\text{TeO}_2$ glass system the refractive index and $\chi^{(3)}$ decrease as the TeO_2 is substituted by the Li_2O , due to the change of TeO_4 trigonal bipyramids into TeO_3 trigonal pyramids. One would then expect that slower structure change in the $\text{PbO}:\text{TiO}_2:\text{TeO}_2$ glasses would result in a slow decrease in the refractive index. Nonetheless the measured values are almost independent of the PbO content. Thus, the presence of the PbO should increase the refractive index to compensate the decrease due to the glass structure change.

CONCLUSIONS

We present highly homogeneous TeO_2 -PbO-TiO₂ glasses with high refractive index. It was found that the Raman peaks to depend on the PbO content. On contrast, the UV-Vis cut-off, optical gap and the linear refractive index were found to be almost independent of the PbO content. These trends are consistent with a glass structure change, with TeO_4 trigonal bipyramids breaking into TeO_3 trigonal pyramids as the PbO content increases. The almost constant refractive indices may be explained by two

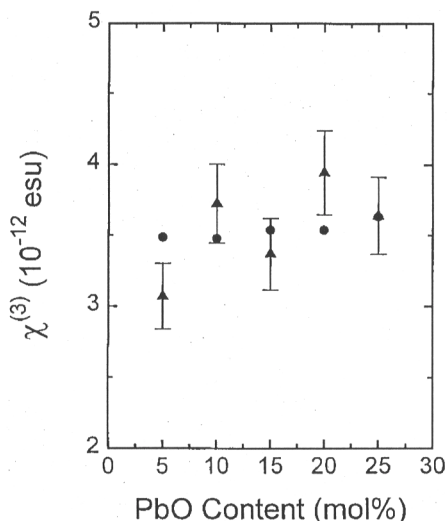


Figure 5. Third order susceptibility $\chi^{(3)}$ as a function of the PbO content for the PTT glass system. The circles represent the data from Yamamoto et al⁶, and the squares are our calculated values.

contributions acting in opposite directions. The PbO itself increases the refractive index, however the increase in PbO content also increases the breaking of TeO₄ trigonal bipyramids into TeO₃ trigonal pyramids, which decreases the refractive index. Nonetheless the $\chi^{(3)}$ values are larger than the pure TeO₂ glasses.

ACKNOWLEDGEMENT

The authors acknowledge the Conselho Nacional de Desenvolvimento Científico e Tecnológico (CNPq), Fundação de

Amparo à Pesquisa do Estado de São Paulo (FAPESP), Programa de Apoio ao Desenvolvimento Científico e Tecnológico (PADCT) and the Telecomunicações Brasileiras S/A (Telebras) for financial supports.

REFERENCES

1. Inoue, S. and Nokui, A.; *Proceedings of the Int. Conf. on Science and Technology of New Glasses*, ed. Sakka S. and Soga, N.; Tokyo, 1991, p. 77.
2. Nasu, H.; Ibara, Y. and Kubodera, K.; *J. Non-Cryst. Solids* **1989**, *110*, 229.
3. Kim, S.-H.; Yoko, T. and Sakka, S.; *J. Am. Ceram. Soc.* **1993**, *76*, 2486.
4. Nasu, H., Matsuhita, O.; Kamyia, H.; Kobayashi, H. and Kubodera, K.; *J. Non-Cryst. Solids* **1990**, *124*, 275.
5. Nasu, H.; Matsuhita, O.; Kamyia, H.; Kobayashi, H. and Kubodera, K.; *Jpn. J. Appl. Phys.* **1992**, *31*, 3899.
6. Yamamoto, H.; Nasu, H.; Matsuoka, J. and Kamiya, K.; *J. Non-Cryst. Solids* **1994**, *170*, 87.
7. Cuevas, R. F.; Barbosa, L. C.; De Paula, A. M.; Liu, Y.; Reinoso, V. C. S.; Alves, O. L.; Aranha, N. and Cesar, C. L.; *J. Non-Cryst. Solids* **1995**, *191*, 107.
8. Khatir, S.; Romain, F.; Portier, J.; Rossignol, S.; Tanguy, B.; Videau, J. J. and Turrel, S. J.; *J. Mol. Struct.* **1993**, *298*, 13.
9. Lines, M. E.; *Phys. Rev. B* **1990**, *41*, 3372; *Phys. Rev. B* **1990**, *41*, 3383.
10. Lines, M. E.; *Phys. Rev. B* **1991**, *43*, 11978.
11. Sekiya, T.; Mochida, N.; Ohtsuka, A. and Tonokawa, M.; *J. Non-Cryst. Solids* **1992**, *144*, 128.
12. Wemple, S. H.; *J. Chem. Phys.* **1977**, *67*, 2151.
13. Nassau, K.; *Electron. Lett* **1981**, *17*, 769; *Bell. Syst. Tech. J.* **1981**, *60*, 327.